*International Journal of Fracture* **108:** 63–72, 2001.


# An examination of small fatigue crack morphology

R. L. CARLSON[1], D. L. STEADMAN[2] and G. A. KARDOMATERS[1]
[1]*School of Aerospace Engineering, Georgia Institute of Technology, Atlanta, Georgia, 30332-0150, USA*
[2]*Delta Airlines, Dept. 572, P. O. Box 20706, Atlanta, Georgia, 30320-6001, USA*

Received 14 December 1998; accepted in revised form 26 October 1999

**Abstract.** Test results for the growth of a small corner crack under cyclic loading are presented. The number of grains that are crossed by the crack front ranges from about three to ten during the crack advance. Crack path profile measurements on the adjacent corner faces are presented. Also, a microscopic examination of the crack path morphology of a polished and etched surface that is adjacent to the corner reveals the presence of complex branching mechanisms, and localized regions of intensive damage. Examination of sub-surfaces reveals that though branching and localized damage are present, they diminish with increasing depth of the subsurface. It is concluded that during early growth, the crack surface deviates substantially from an idealized planar surface model, and that Modes I, II, and III are all operative.

**Key words:** Aluminum alloy, crack morphology, crack path profiles, microstructure, Modes I, II, III, short cracks, scatter, small cracks.

## 1. Introduction

The objective of predictive codes for fatigue crack growth is to provide estimates of the lives of structural components. Currently, the codes are formulated to account for threshold effects, closure effects and the value of the critical stress intensity factor. The predictive capabilities of these codes have generally been found to be quite acceptable for what have been characterized as 'long' cracks, e.g., for crack lengths which are an order of magnitude larger than a microstructural feature such as grain size. It is known, however, that the phases of the total fatigue life that consume a substantial part of the life are associated with the nucleation and the initial, small crack growth regimes. Initial studies of small crack growth have often focused on experimental observations that the growth rate of small cracks is greater than that of long cracks for the same range of stress intensity factor. This has been characterized as an anomalous behavior. A frequent explanation for this behavior has been that small cracks do not encounter as much closure obstruction as long cracks, and as a consequence, more of the applied range of stress intensity factors is effective in producing growth. This has led Liaw and Logsdon (1985) and Edwards and Newman (1990) to introduce the use 'effective' ranges of stress intensity factors.

Two other important features of the growth behavior have also been observed. These are intervals of arrested crack advance, and a lack of reproducibility or scatter in repeated experiments. Both of these features have been observed by Carlson et al. (1997) and by Carlson and Halliday (1998) to occur when the number of grains intersected by the crack front is small. Effective stress intensity factors cannot, however, account for either of these features.

One objective of this paper is to present experimental results which describe the evolution of a small fatigue crack surface which differs substantially from the planar surfaces which

are assumed in fracture mechanics based analyses. A second objective is to examine the implications of the observed features.

## 2. Experimental details

A small, corner crack growth experiment was conducted on a 6061-T651 aluminum alloy specimen which was machined from 16 mm diameter bar stock. The average transverse intercept grain size was 200 microns, and the average longitudinal intercept grain size varied widely about an average of 350 microns. The 0.2% offset yield stress was 283 MPa, and the ultimate strength was 293 MPa. A three point, sinusoidally applied bending load. The load ratio was $R = 0.0625$. The cross-section in the gage section was a square with 10.2 mm sides, and it was oriented to produce a maximum tensile stress at a mid-point corner. That is, the neutral axis coincided with a cross-section diagonal. At this location, a small notch with a 60-deg included angle was introduced using a digitally controlled slitting saw. The bottom edge of the notch was normal to the axis of the specimen. After notching, the faces adjacent to the notch were prepared for testing by the use of five grades of abrasive paper which ranged from 600 to 2000 grit. Polishing was completed by the use of 3 and 1 micron diamond paste. The notch depth after polishing was 60 microns.

The fatigue crack growth test was conducted on an Instron servo hydraulic testing machine under sinusoidal loading at 10 Hz. A telemicroscope system was used to monitor crack growth. Measurements were obtained for both sides of the corner. Details of the experimental measurement system have been described in a previous publication (Carlson et al., 1996). Cracks were initiated on both sides of the notch by the application of a nominal maximum stress of 0.9 of the yield stress. After crack initiation, the maximum load was reduced to produce a nominal maximum stress of 0.55 of the yield stress. Crack length measurements included the notch depth of 60 microns. When the crack lengths were about 1400 microns, the test was discontinued. At the beginning of the crack length measurements, the number of grains crossed by the crack front was about three. It has been previously observed (Carlson et al., 1996) that at the end of the measurements, the number of grains, which were crossed by the crack front, was about ten. Plots of the crack growth histories on the two adjacent corner faces are represented in Fig. 1 by the symbols A and B.

Crack path features were examined by two procedures. In the first a telemicroscope was used to create crack profile maps for both corner faces. The results of these measurements are presented in Figure 2. For these measurements the specimen was statically loaded to open the cracks slightly. The $x$ axis coordinate values represent the locations in the crack growth directions, and they include the notch depth, which was 60 microns. The $y$ coordinate values represent the deviations from a plane normal to the corner edge. The $y$ coordinate values were measured at 30 micron increments in the $x$ axis direction. Measurements for the left face, which corresponds to the side B of Figure 1, are indicated as negative values of $x$. Measurements for the right face, which corresponds to the side A of Figure 1, are for positive values.

The method used to examine crack morphology consisted of microscopically examining, first the outer crack face of the A surface, and then, by successively removing layers parallel to that surface, examining crack growth features beneath the outer surface. This procedure began by embedding a 13mm section in the center of the gage length in Bakelite. The cracked outer surface was then polished using paper, 3micron grit, and suspended aluminum oxide

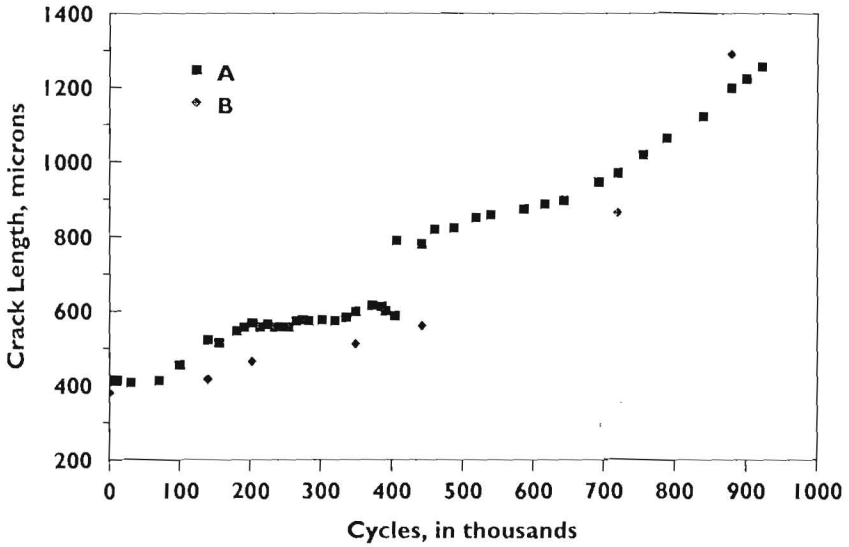


*Figure 1.* Corner crack lengths versus loading cycles on adjacent faces A and B.

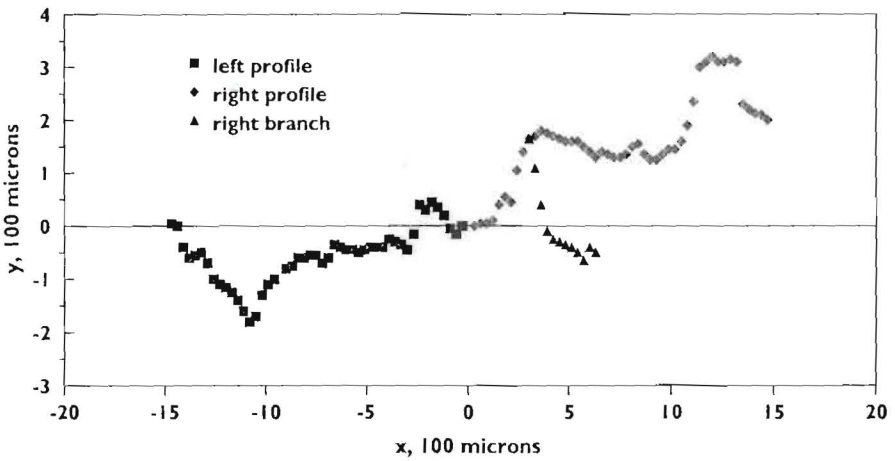


*Figure 2.* Crack path profiles on adjacent corner faces A and B. The insert br represents branching, gb represents grain boundary and dm represents damage.

in preparation for microscopic examination. The outer surface was then etched with Kellers solution to reveal grain boundaries. Three layers were then removed with 1400 grit paper. The polishing procedure was then repeated for each plane. The thickness of each removed layer was about 250 microns. The crack path on the face of each subsurface was microscopically examined. Note that the corner crack, in contrast to a surface crack, can be readily examined by the above procedure. Results of these examinations are presented in Figures 3–5. The features displayed by the crack growth histories, the crack profile maps and the microscopical photographs are discussed in the next section.

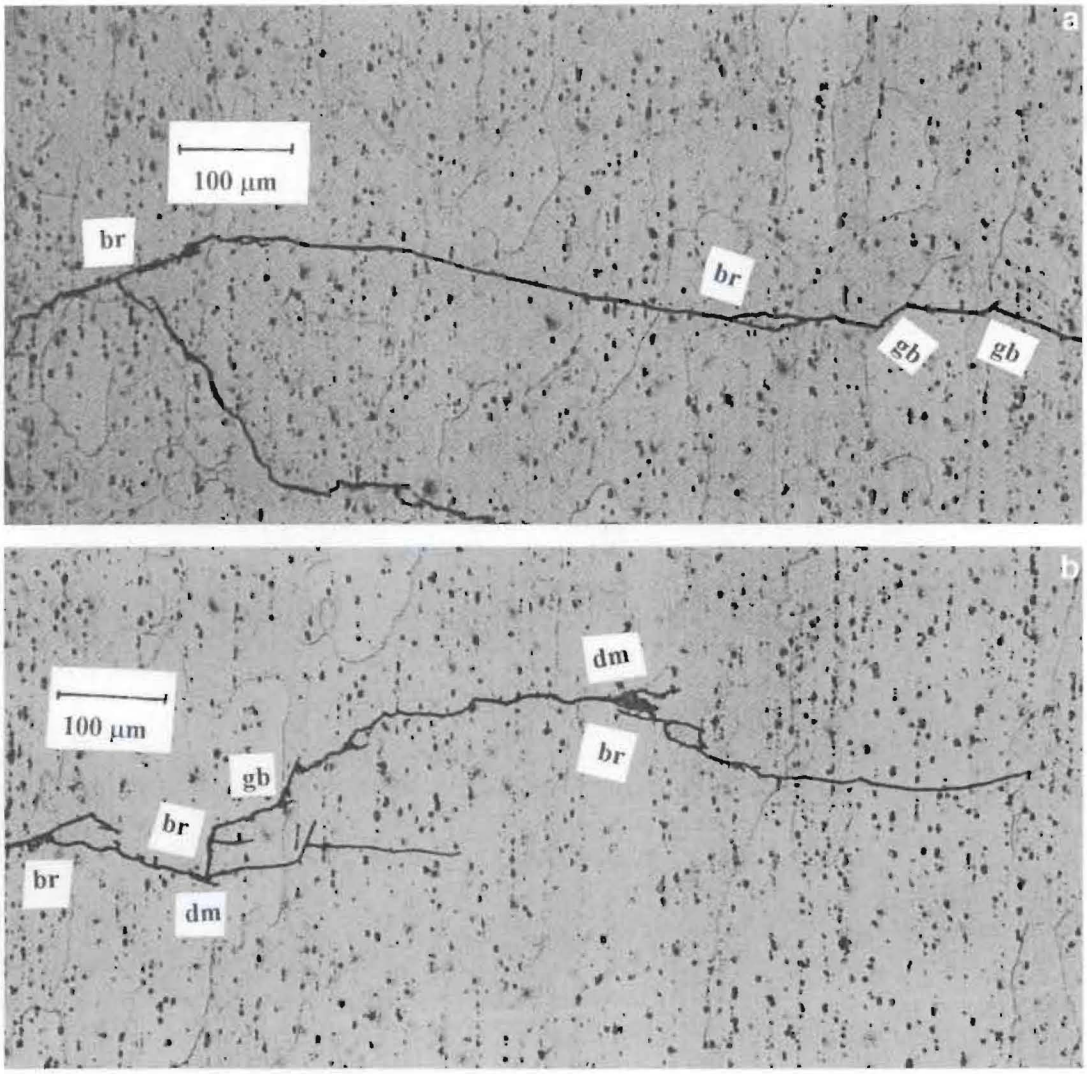


*Figure 3.* a. Crack path on the polished and etched face of side A. b. Continuation of the crack shown Figure 3(a).

## 3. Discussion

The crack growth history in Figure 1 displays features which have been previously observed (Carlson et al., 1998) for two additional specimens tested under the same loading conditions. The growth arrest behavior was present in each of the tests in which the number of grains intersected by the crack fronts ranged from about three to ten. Substantial scatter was present over the entire range of crack growth for the three tests, i.e., the reproducibility associated with long crack growth had not been achieved for these tests.

Recently, results of an application of the Student t distribution were presented by Carlson and Halliday (1998) for the same type of specimen, but for $R = 0.2$ and a maximum stress of 0.8 of the yield stress. They observed an abrupt decrease in the 95 per cent confidence interval as the number of grains intersected by the crack front increased from about three to about six. At the lower end, about 75000 cycles, the variation in the deviation of the crack length

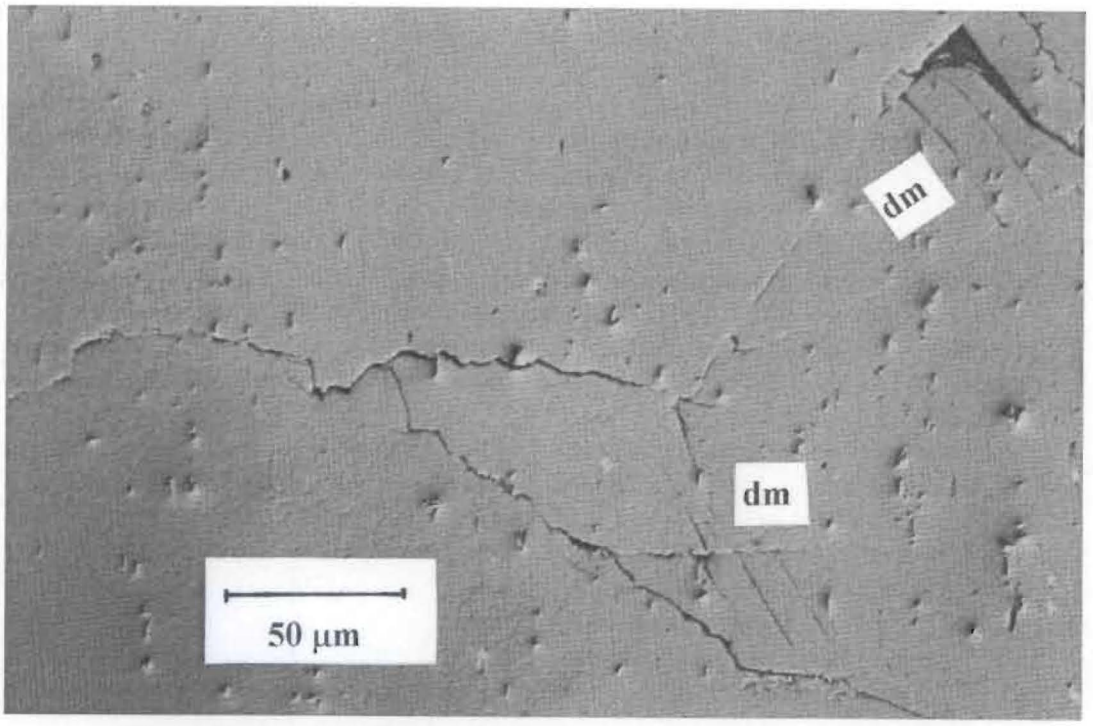


*Figure 4.* Crack path on polished plane 350 microns below the outer surface of Figure 3.

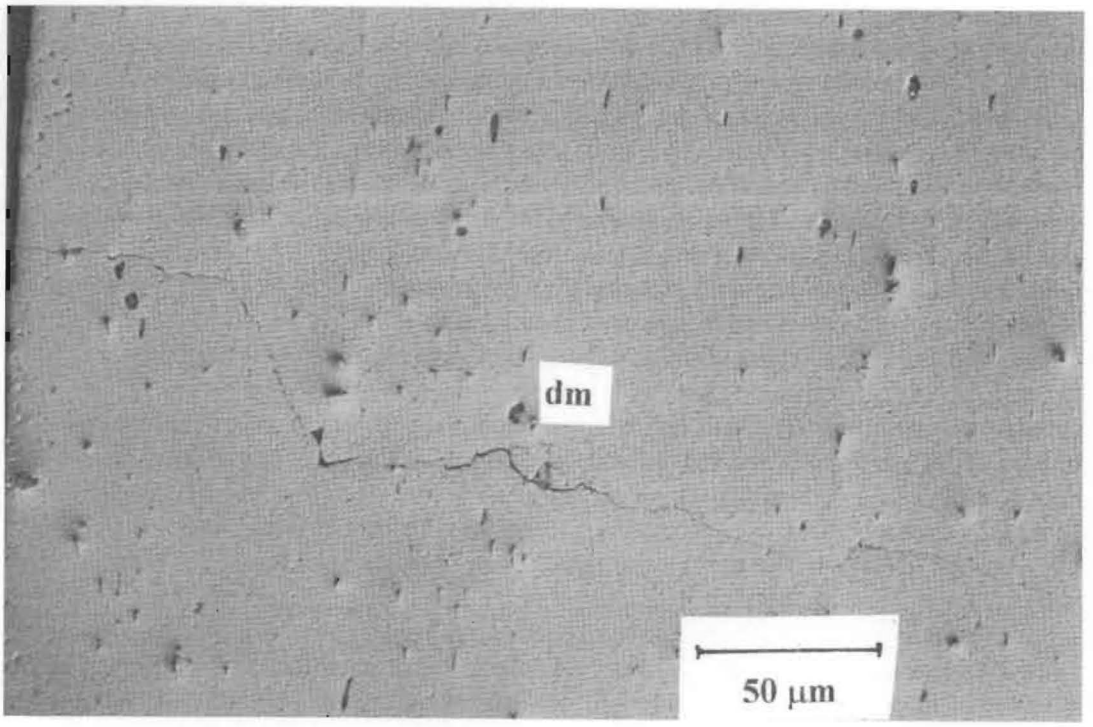


*Figure 5.* Crack path on a polished plane 750 microns below the outer surface of Figure 3.

from the sample mean was ±50%. At the upper end, about 250 000 cycles, the deviation was about ±6%. This indicates that a transition crack length from irreproducible to reproducible growth is dependent on grain size. The results cited in the preceding paragraph (Carlson et al., 1998) were for $R = 0.0625$, and a maximum stress of 0.55 of the yield stress, and they exhibited substantial scatter throughout a similar range of crack lengths. It may, therefore, be concluded that the magnitude of the applied loading must also be a factor. The difference in the ranges of irreproducibility for these two cases may be attributed to an expectation that the larger maximum stress could more easily overcome grain boundary barriers during crack advance.

As can be seen in Figure 2, the crack path segments lie both above and below the main fracture plane. One feature of the crack profile maps which should be noted is the indicated development of branching on face A which is in the positive x direction. Note that, ultimately, one of the paths arrests.

Possible insight into the growth mechanisms which led to the abrupt jump in crack length which occurred in Figure 1 at about 400 000 load cycles can be gained by reference to the crack profile maps of Figure 2. The results suggest that, initially, the cracks on the two faces were separate cracks that joined to form a dominant, single crack. Recently, Carlson and Halliday (1998) presented results for small surface cracks in the aluminum alloy 2024-T351. At a typical site cracks emerged from two edges of a cracked inter-metallic particle. Growth emerged from the particle in significantly different directions on the two sides. Also, the crack on one side grew much faster than that on the other side. The observed behavior in this case was attributed to the fact that the particle was on a grain boundary so that the cracks had grown into two separate grains.

The initial y value deviations of the crack paths from the main fracture plane in Figure 2 are in some parts quite substantial when compared to the projected crack length. This indicates that, on this scale, where only a few grains are encountered by the crack front, local representations of the crack surface should be three-dimensional. That observation follows since the crack profiles on the two outer faces differ, interior crack profiles on radial planes must change between the two outer surfaces. Also, since crack surface segments are inclined to the main fracture plane, it can be concluded that, locally, Modes I, II and III would be present, and that they would vary along the crack front. For long cracks with long crack fronts the effects of these local, microscopic deviations are effectively averaged out.

Although the results presented in Figure 2 are informative, they do not provide descriptions of microscopic mechanisms that produced the observed crack profiles. The photographs of Figures 3–5 provide this type of information. Figures 3(a) and 3(b) are photomicrographs of the polished and etched outer surface that has been identified in Figure 1 as side A. These photographs provide a description of the entire crack length. Several features are of interest. Clearly, the crack deviates from a straight path, and many small, abrupt changes in direction can be observed. Grain boundaries are present at some of these direction changes, and some of these have been indicated by the insert gb. Also of interest are instances in which branching has occurred. These have been indicated by the insert br. Note that a few of the branches have rejoined to form loops after a short distance.

Of special interest are two locations where complex patterns of cracking have occurred. These appear as a form of highly localized damage and they have been indicated by the insert dm. The features associated with this type of damage are similar to those which have been described by Petit (1992) for an Al-4.6 Cu-1.1 Li-Zr alloy.

Examination of polished sub-surfaces revealed that crack path deviations and branching diminished as the depth of the exposed surface increased. Patches of localized damage were, however, still observed. Two damaged sites for the first sub-surface, which was about 250 microns below the original surface, are indicated by the insert dm in Figure 4. These sites were about 500 microns from the corner of the specimen. The 'shattering' at these locations resembles the networks of localized fracture that occur in brittle materials.

A less intensive damage site is indicated in Figure 5. This site was located about 750 microns below the original, exterior surface, and about 770 microns from the specimen corner. The decrease in the amounts of branching and local damage with increasing depth below the outer surface is likely to be related to the fact that slip in partially constrained, surface grains is easier than in fully constrained, interior grains. The consequences of this on small fatigue crack growth are examined later in this section.

Since grain pattern distributions cannot be expected to be the same at all locations where small cracks are growing, the growth behaviors can be expected to result in a lack of reproducibility in repeated tests. Scatter in two aluminum alloys (Carlson and Halliday, 1998) was described earlier in this paper.

A thorough examination of scatter under both laboratory and service conditions has been presented in a comprehensive paper by Schijve (1994). Such considerations indicate that a statistical representation of growth in the small crack regime is necessary. To account for the statistical aspects of the growth, Cox and Morris (1988) have generated a random, two-dimensional pattern of grains, and presented a Monte Carlo simulation of small cracks growing under mode I cyclic loading through stochastically produced microstructures. To represent the observed growth arrest behavior, Steadman et al. (1998) introduced the use of 'graftals' that had previously been used by Smith (1984) to describe growth in biological systems. For the algorithm developed the fracture plane was discretized into a pattern of concentric rings which were composed of individual tiles. The conditions required for crack advance at each tile were stochastically controlled by 'trapping' and 'untrapping' rules. Stress intensity factors that were dependent on local shape were computed by use of results obtained by Murakami and Nemat-Nasser (1983).

Local, effective stress intensity factors based on isotropic elasticity were used for both of the above models, so varying crystallographic orientations are not accounted for. Although the analyses were two dimensional, lying in a flat plane of the crack advance, Cox and Morris (1988) suggested that three dimensional effects could be incorporated by the use of out-of-plane crack deflection results of the type formulated by Suresh (1991).

The types of branching and the forms of localized damage observed here are very complex. Also, the types of grain shapes encountered in service components can, depending on the type of processing used, vary widely, e.g., elongated, pancake, etc. For these examples the local directions of crack propagation can also be expected to introduce further complications. To incorporate all of the features of the small crack growth process, it may be necessary to base statistical models on results from experiments in which specimens that duplicate the microstructures, and crack geometry of given components are tested.

Leis et al. (1986) have suggested that another aspect of small fatigue crack growth should be recognized as having a possible effect on the growth behavior. This is associated with the fact that the ratio of the number of fully constrained, interior grains to the number of partially constrained, surface grains is much larger for long cracks than it is for small cracks. Recently, Carlson et al. (1997) suggested that the differences in this ratio may produce differences in the growth behavior of small corner cracks, small surface cracks and short surface cracks. The

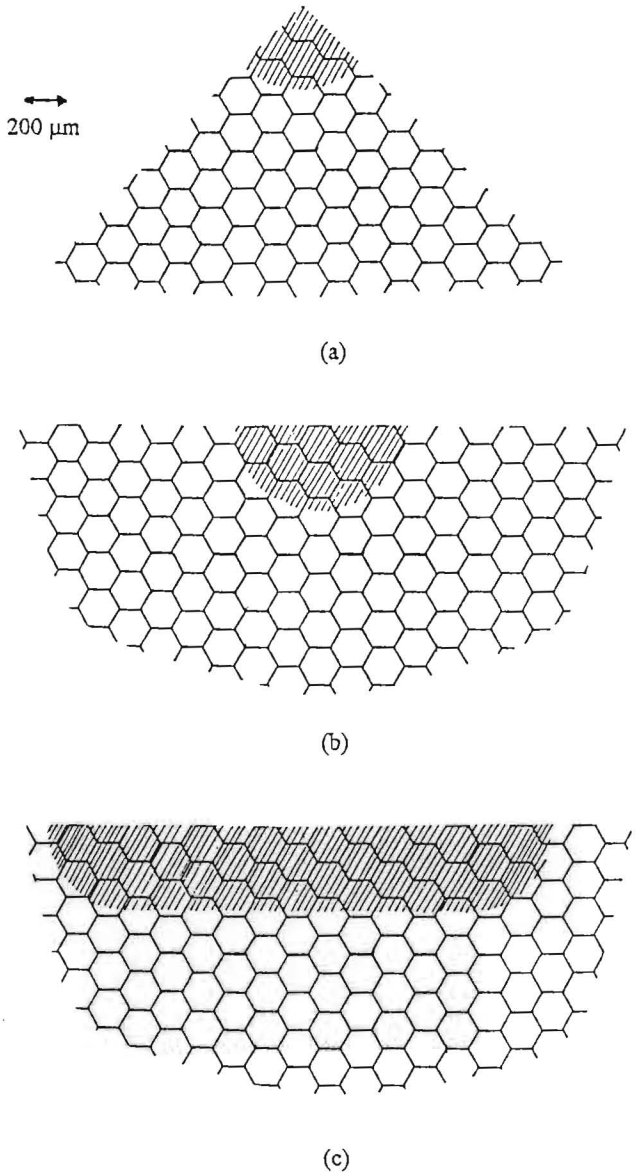


*Figure 6.* Crack surface representations for (a) small corner crack, (b) a small surface crack and (c) a short surface crack.

differences in the ratios for these three types of cracks are illustrated in Figure 6 by arrays of 200 micron, hexagonal grains. The shaded areas represent cracks of the same depth in a small corner crack, a small surface crack and a short surface crack. Note that all of the dimensions of the small corner crack and the small surface crack are small, whereas only the depth dimension of the short surface crack is small. Small surface cracks have been initiated by cyclic, tensile loading. Short surface cracks may be developed in a plate under cyclic bending due to the stress gradient. An examination of the figures for the given crack depth indicates that the ratios of the number of grains crossed by the crack front to the number of surface grains crossed by the crack front range from about 2.5 to 5 to 9.5, respectively, for the three cases. Although the

ratio of interior to surface grains for the short surface crack differs from the other two most significantly, the ratios of the small corner crack and the small surface crack can be expected to differ by a factor of about two. Slip in partially constrained surface grains is easier than in fully constrained interior grains. See, for example, the differences in the features of crack advance for surface grains in Figure 3, and interior grains in Figures 4 and 5. It follows that the initial growth behavior, including scatter, for these three types of cracks in Figure 6 may be expected to differ. Note that the stress intensity factor does not account for these constraint effects.

The above considerations apply in the regime in which crack lengths are of the order of the grain size; that is, soon after crack initiation. The importance of being able to characterize small crack parameters soon after crack initiation has been recognized recently by Torng and McClung (1994). After reviewing probabilistic methods for representing scatter in fatigue, they proposed a method based on the use of data from $da/dN$ versus effective $\Delta K$ plots. They modified a lognormal, random variable model proposed by Yang et al. (1985) to account for the increase in variability in the small crack regime. The ultimate objective of their method was to provide a procedure for predicting confidence limits for crack growth from the small crack regime into the long crack regime. To start their analysis, non-zero, initial values of crack length and load cycle had to be selected. In applying their method to HSLA-8 steel they found that the derived confidence limits were not good in the small crack regime. They concluded that their results revealed the importance of the selection of the initial values of crack length and load cycle.

## 4. Conclusions

The surfaces of the small corner cracks deviate significantly from the idealized model representations assumed in analyses. Modes I, II and III can all be expected to be operative during early growth. Complex forms of crack branching and highly localized regions of substantial damage develop as the crack propagates. Reproducibility should not be expected when the number of grains crossed by a crack front is small. Codes for predicting small fatigue crack growth should be based on statistical representations that are derived from tests on specimens that incorporate microstructural features and small crack geometry.

## Acknowledgement

The authors would like to acknowledge the help of Carter Hamilton who contributed valuable assistance in the metallography work.

## References

Carlson, R.L., Steadman, D.L., Dancila, D.S.and Kardomateas, G.A. (1996).An investigation of the growth of small corner cracks from small flaws in aluminum 6061-T651. *Proc.Sixth International Fatigue Congress*, (Edited by G.Lütjering and H. Nowack), 289–294.

Carlson, R.L., Steadman, D.L., Dancila, D.S.and Kardomateas, G.A. (1997). Fatigue growth of small corner cracks in aluminum 6061-T651. *International Journal of Fatigue* **19**, 119–125.

Carlson, R.L., Steadman, D.L.Dancila, D.S.and Kardomateas, G.A. (1998). An experimental investigation of the growth of small corner fatigue cracks in aluminum 6061-T651. *Fatigue and Fracture of Engineering Materials and Structures* **21**, 403–409.

Carlson, R.L.and Halliday, M.D. (1998). *A Consideration of Scatter in Small Fatigue Crack Growth. Low Cycle Fatigue and Elasto-Plastic Behaviour of Materials* (Edited by K.T.Rie and P.D. Portella), Elsevier, 511–516.

Cox, B.N.and Morris, W.L. (1988). Monte Carlo simulations of the growth of small fatigue cracks. *Engineering Fracture Mechanics* **31**, 591–610.

Edwards, P.R.and Newman Jr, J.C. (1990). An AGARD supplemental test program on the behavior of short cracks under constant amplitude and aircraft spectrum loading. *Short Crack Growth in Various Aircraft Materials*. AGARD REPORT 767.

Leis, B.N., Hopper,A.T., Ahmad, J., Brock, D.and Kanninen, M.F. (1986). Critical review of the fatigue growth of short cracks. *Engineering Fracture Mechanics* **23**, 883–898.

Liaw, P.K. and Logsdon, W.A. (1985). Crack closure: an explanation for small fatigue crack growth behavior. *Engineering Fracture Mechanics* **22**, 115–121.

Murakami, Y.and Nemat-Nasser, S. (1983). Growth and stability of interacting flaws of arbitrary shape. *Engineering Fracture Mechanics* **17**, 193–210.

Petit, J. (1992). *Modeling of Intrinsic Fatigue Crack Propagation, Theoretical Concepts and Numerical Analysis of Fatigue* (Edited by A.F. Blom and C.J. Beevers), Engineering Materials Advisory Services LTD., Warley, West Midlands, UK, 131–152.

Schijve, J. (1994). Fatigue predictions and scatter. *Fatigue and Fracture of Engineering Materials and Structures* **17**, 381–396.

Smith, A.R. (1984). Plants, fractals and formal languages. *Computer Graphics* **18**, 1–10.

Steadman, D.L., Carlson, R.L.and Kardomateas, G. A. (1998). Expert system model of small crack growth. *Proc. 39th AIAA/ASME/AHS/ASC Structures and Materials Conf.* Part 4, 3003–3013.

Suresh, S. (1991). *Fatigue of Materials*, Cambridge University Press, 182–189.

Torng, T.Y. and McClung, R.C. (1994). Probabilistic fatigue life prediction methods for small and large fatigue cracks. *Proc. 35th SDM Conference, AIAA*, 1514–1525.

Yang, J.N., Hsi, W.H. and Manning, S.D. (1985). *Stochastic Crack Propagation with Applications to Durability and Damage Tolerance Analysis*, AFWAL-TR-85-3062.